

# Thermal conductivity and thermal contact conductance studies on $\text{Al}_2\text{O}_3/\text{Al}-\text{AlN}$ metal matrix composite

V.V. Rao, M.V. Krishna Murthy, J. Nagaraju \*

*Department of Instrumentation, Indian Institute of Science, Bangalore 560 012, India*

Received 10 June 2003; received in revised form 20 April 2004; accepted 10 May 2004

Available online 6 July 2004

---

## Abstract

$\text{Al}_2\text{O}_3/\text{Al}-\text{AlN}$  is a metal matrix composite (MMC) used for making heat sink of electronic devices. This paper presents the detailed investigations carried out on thermal contact resistance across this MMC contact in vacuum at different contact pressures. The experimental results are compared with the theoretical models available in the literature for metallic contacts and they are found to be in good agreement with each other.

**Keywords:** A. Metal matrix composite; Thermal conductivity

---

## 1. Introduction

The progress and developments in the materials technology have resulted in several new materials like metal matrix composites (MMCs) designed to suit specific requirement. MMCs possess the combined properties of metals as well as the ceramics. These MMCs are characterized by some excellent mechanical properties (high mechanical strength and low weight) and thermal properties (high thermal conductivity and low thermal expansion), which make them a suitable candidate for thermal management applications. Heat sink used in electronic devices is an example for  $\text{Al}_2\text{O}_3/(\text{Al}-\text{AlN})$  metal matrix composites. A lack of knowledge concerning the characteristics of these new materials often hinders their wider utilization. Thus the need for determination of the properties like thermal conductivity and thermal contact conductance arises often.

When two solid surfaces are brought into contact with each other for the purpose of transmitting energy in the form of heat, the interface formed between them is known as a contact. An extra resistance offered at the interface, when heat transfer takes place across the interface, is known as thermal contact resistance ( $R_c$ ). Thus  $R_c = \Delta T/Q$  and the thermal contact conductance  $h_c = Q/A_a \Delta T$ , where  $Q$  is the heat flow rate,  $\Delta T$  is the interface temperature drop and  $A_a$  is apparent contact area. Mikic [1] investigated theoretically the effect of mode of deformation on the predicted values of thermal contact conductance and suggested a correlation for plastic and elastic deformation. Sridhar and Yovanovich [2] proposed an elasto-plastic contact-conductance model for isotropic and conforming rough surfaces. Jeng et al. [3] studied the effect of mode of deformation of surface asperities on thermal contact conductance. Aikawa and Winer [4] measured the thermal contact conductance across sintered silicon nitride disk type contacts and observed that the thermal contact conductance is proportional with the applied contact pressure when their logarithmic values are plotted. Chung et al.

---

\* Corresponding author. Tel.: +91-80-2293-2273; fax: +91-80-2360-0135.

E-mail address: [solarjnr@isu.iisc.ernet.in](mailto:solarjnr@isu.iisc.ernet.in) (J. Nagaraju).

[5] conducted experiments on Aluminum (6061-T651) substrates coated with Cu, Al, Al plus Cr and Iron carbide and observed that the contact conductance is higher with Al plus copper coated contacts than the other three coated contacts. Lambert and Fletcher [6] measured the thermal conductivity of graphite fiber reinforced aluminum and copper metal matrix composites. Rao et al. [7] measured the thermal contact resistance across Al12%Si10wt%SiC<sub>p</sub> MMCs.

## 2. Experimentation

The experimental setup (shown in Fig. 1) consists of a contact conductance cell, a hydraulic loading unit, a heating circuit, a cooling circuit, a vacuum system and instrumentation. The test column assembly consists of a pair of heater-cooler blocks, test specimens, heat flux meters made of OFHC copper and a ball-cone seating arrangement on either side. The heater-cooler block can be used either as a heater or as a cooler. A triple-walled chamber made of SS304 accommodates the test column and is designed to withstand a vacuum of  $5 \times 10^{-6}$  Torr. Loading system consists of a hydraulic power pack, a hydraulic jack, a compression-type load cell, and a digital load indicator. The test setup is equipped with the necessary instrumentation like electrical wattmeter, vacuum gauges, data acquisition system etc., for the measure-

ment of various parameters. Detailed description of the complete test set up is given in [8].

$\text{Al}_2\text{O}_3/\text{Al}-\text{AIN}$  MMC is prepared by pressure less infiltration of Al-6Mg-6Si-0.3Fe alloy into porous preforms of alumina. The preforms are made by uniaxially pressing the alumina powder (average size 23  $\mu\text{m}$ ) into cylindrical shapes of 25 mm diameter and sintering at 1300 °C for 2 h to a theoretical density of 55%. For heat treatment these preforms were placed over the alloy billet in a graphite crucible and the whole assembly was in turn placed in a tube furnace. The furnace temperature was raised to 900 °C and maintained there for 8 h to allow for the complete infiltration of the preforms by the alloy and furnace cooled to the room temperature.

Each specimen is ground on a machine to a cylinder of 25 mm length and 25 mm diameter. The form ratio (length to radius) of the sample is 2. Three holes, to accommodate thermocouples, at a distance of 6.25 mm are drilled in each specimen along the radial direction to a depth of 12.5 mm from the surface. The hole diameter is 1.2 mm and therefore, the hole depth to diameter ratio is 10. The surfaces of the specimens are prepared with fine polished paper. The specimen surfaces are cleaned in an ultrasonic bath to remove the dirt and they are further cleaned with acetone and then with isopropyl alcohol. The surface characteristics (rms roughness- $\sigma$ , and mean absolute slope- $m$ ) of two contacting surfaces are measured using a stylus based Form Talysurf-5 instrument and the values are given below:

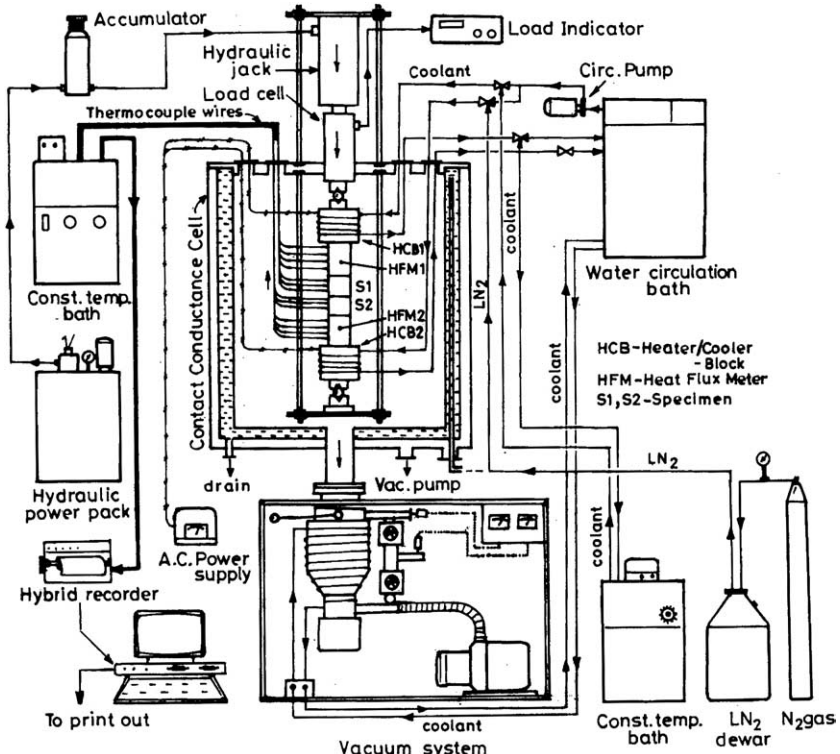


Fig. 1. Experimental setup.

Specimen-1	$\sigma = 0.5787 \mu\text{m}$	$m = 0.0333$
Specimen-2	$\sigma = 0.5637 \mu\text{m}$	$m = 0.1933$

Before mounting the specimens in test column, the micro-hardness of material is tested using a Vickers micro-hardness tester (HMV 2000 Shimadzu). Thermal grease is applied to all the interfaces except for the test interfaces in order to enhance the heat transfer through the test column. The specimens and the heat flux meters are inserted in a Teflon tube to ensure axial alignment as well as to reduce the radial heat losses. Thermocouple junctions are fitted in the hole drilled on the test specimens and the heat flux meters using a heat sink compound. The experimental procedure followed is as follows: The contact conductance cell and is evacuated to a pressure of  $10^{-5}$  Torr after mounting the test column inside it. The hydraulic pump is started. The solenoid valve that acts as a pressure switch is dethrottled. The load indicator is energized and adjusted to read zero with no load. The solenoid valve is throttled to increase the pressure on the samples. The entire system is kept on for 12 h and is allowed to reach the steady state condition. Data were taken when the test specimen temperatures did not vary by more than  $0.2^\circ\text{C}$  over a one-hour period. These data were used to determine the temperature gradients and the heat flux in the test specimens. Then the heater current is increased to a higher value such that the heat flux through the test column increases. This procedure is repeated to find the thermal conductivity of the specimens at various mean bulk temperatures. The heat flux values in the heat flux meters can be calculated using the temperature gradient obtained by a linear least squares fit and the thermal conductivity of the heat flux meter material. Fourier's law of heat conduction is used to determine the thermal conductivity of the test specimens from the measured heat flux and the known specimen dimensions. The top heat flux meter gives the heat supplied to the test specimen and the bottom heat flux meter gives the heat removed from the test specimen. It is observed that the heat flux in the top flux meter is more than that in the bottom flux meter. This is due to the radiation from the column. For all heat inputs, the heat flux values obtained from the two heat flux meters differed by less than 3%. This shows that the heat flow in the test column is nearly one-dimensional and the radial conduction heat losses are negligible. For calculations, the average heat flux value is used. The effect of the applied contact pressure on the test interface is studied by increasing the load in steps of 100–1000 kg. The steady state temperature values are recorded for every load. Thus the experiments were conducted across MMC contacts in vacuum by varying the contact pressure as well as varying the heat input for each value of contact pressure.

### 3. Results and discussion

Thermal conductivity of  $\text{Al}_2\text{O}_3/\text{Al-AlN}$  (MMC) at different temperatures is shown in Fig. 2. These measured values are as per the following correlation

$$k(\text{W/m K}) = [-0.0591]T + 57.62; \quad 40^\circ\text{C} < T < 150^\circ\text{C}$$

Thermal conductivity of MMC decreases marginally with the increase in temperature up to  $150^\circ\text{C}$ . Lambart and Fletcher [6] reported that the thermal conductivity of graphite fiber reinforced aluminum and copper metal matrix composites do not vary with temperature in the range  $20$ – $146^\circ\text{C}$ .

Fig. 3 shows the variation in interface temperature drop and heat flow rate in the test column with contact pressure. The interface temperature drop decreases with contact pressure whereas the heat flow rate almost remains constant.

In order to compare the experimental data on thermal contact conductance with the theoretical models, a graph between dimensionless contact conductance versus dimensional contact pressure is plotted and shown in Fig. 4. The contact conductance is made dimensionless by multiplying with the surface roughness ( $\sigma$ ) and

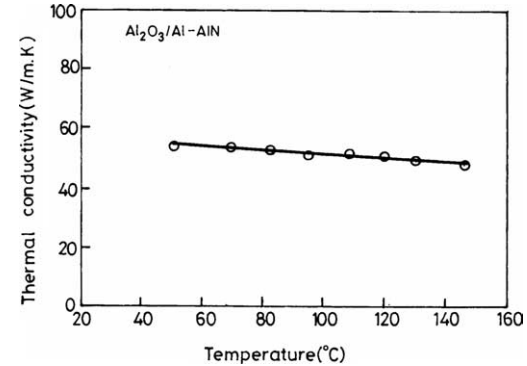


Fig. 2. Variation of thermal conductivity with temperature.

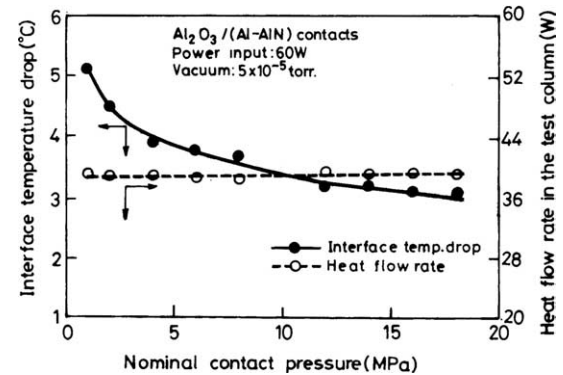


Fig. 3. The variation of interface temperature drop and the heat flow rate with contact pressure.

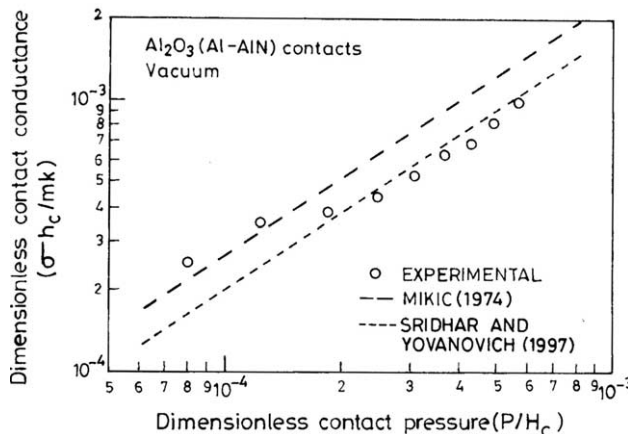


Fig. 4. Comparison of experimental and theoretical values of contact conductance.

dividing it with mean surface slope ( $m$ ) and thermal conductivity of the sample ( $k$ ). The contact pressure is also presented in a dimensionless form by dividing the contact pressure ( $P$ ) with the material hardness ( $H$ ). The measured thermal contact conductance values are higher than both the theoretical model values at low contact pressures and in good agreement at high contact pressures. It is requisite to mention here that the theoretical models given in [1,2] are derived for metallic contacts and many researchers have found that these are more accurate at higher contact pressures. Both the models tend to under predict the thermal contact conductance values at relatively low contact pressures.

Figs. 5 and 6 show the variation of thermal contact conductance with heat flow rate and mean interface temperature, respectively. TCC exhibits a weak dependence on the heat flow rate and consequently on the mean interface temperature. This is because the interface temperature drop ( $\Delta T$ ) also increases with the increase in heat flow rate and thereby the mean interface temperature. This rise in  $\Delta T$  counter acts for the rise

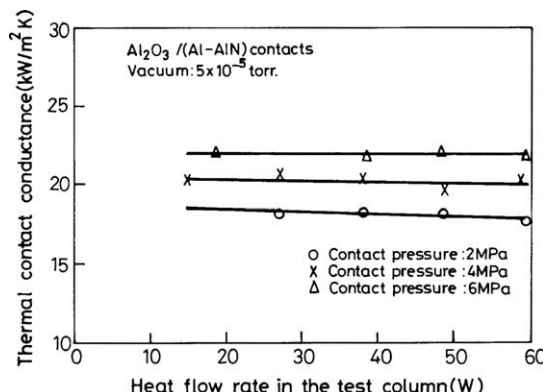


Fig. 5. Variation of thermal contact conductance with heat flow rate.

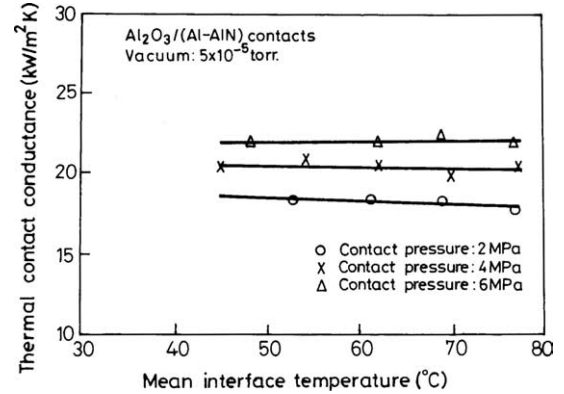


Fig. 6. Variation of thermal contact conductance with interface face temperature.

in heat flow rate and results in a relative invariance in TCC. Hence, it can be concluded that the TCC is independent of thermal conductivity of the contact material.

#### 4. Conclusions

The experimental investigations conducted on  $\text{Al}_2\text{O}_3/\text{Al}-\text{AlN}$  MMCs show that thermal contact conductance increases, as a function of contact pressure and it is a weak function of mean interface temperature. The theoretical models suggested for metallic contacts can be used for predicting the thermal contact conductance of  $\text{Al}_2\text{O}_3/\text{Al}-\text{AlN}$  metal matrix composites with reasonably good accuracy.

#### References

- [1] Mikic BB. Thermal contact conductance theoretical considerations. *Int J Heat Mass Transfer* 1974;17:205.
- [2] Sridhar MR, Yovanovich MM. Elastoplastic contact conductance model for isotropic uniform rough surfaces and comparison with experiments. *Trans ASME J Heat Transfer* 1996;118:3.
- [3] Yeau-Ren Jeng, Chen JT, Cheng CY. Theoretical and experimental study of a thermal contact conductance model for elastic, elastoplastic and plastic deformation of rough surfaces. *Tribology Lett* 2003;14(4):251.
- [4] Aikawa T, Winer WO. Thermal contact conductance across Si/sub3/N/sub4/-Si/sub33/Nsub4/contact. *Wear* 1994;177:25.
- [5] Chung KC, Benson HK, Sheffield JW. Thermal contact conductance of ceramic substrate junctions. *Trans ASME J Heat Transfer* 1995;117:508.
- [6] Lambert MA, Fletcher LS. Thermal conductivity of graphite/copper composites. *Trans ASME J Heat Transfer* 1996;118:478.
- [7] Rao VV, Nagaraju J, Krishna Murthy MV. Thermal conductivity and thermal contact conductance studies on Al12%-Si10wt%SiC<sub>p</sub> metal matrix composites. *J Compos Mater* 2003;37(19):1713.
- [8] Rao VV, Bapurao K, Nagaraju J, Krishna Murthy MV. Instrumentation to measure thermal contact resistance. *Meas Sci Technol* 2004;15:1.